Supplemental Information

Solution structure and functional importance of a conserved RNA hairpin of eel LINE UnaL2

Yusuke Nomura, Masaki Kajikawa, Seiki Baba, Shinta Nakazato, Takayuki Imai, Taiichi Sakamoto, Norihiro Okada, and Gota Kawai*

*Corresponding author

Department of Life and Environmental Sciences, Faculty of Engineering, Chiba Institute of Technology, 2-17-1 Tsudanuma, Narashino, Chiba 275-0016, Japan

Phone & Fax: +81-47-478-0425.

E-mail address: gkawai@sea.it-chiba.ac.jp

1. Structure and dynamics of LINE36 mutants

Here, the structures of LINE36 mutants corresponding to those used for the retrotransposition assay (Fig. 6 in the manuscript) were analyzed by NMR and the thermal stabilities of the mutants were analyzed by the UV-melting experiment.

Materials and Methods

RNA synthesis, purification, and preparation - For structural determination, non-labeled LINE36 mutants C8U, C8A, C8G, C8del, C8CC and U28A were prepared as described in the manuscript

NMR measurements of LINE36 and its mutants - NMR spectra were measured using Bruker DRX-500 and DRX-600 spectrometers. Spectra were recorded at probe temperatures of 4-10 °C were used for structural analysis. Exchangeable proton resonances were assigned by NOESY in H_2O with mixing times of 150 ms using the jump-and-return scheme for water suppression.

Melting profiles measurements of LINE36 and its mutants - The absorbance was measured at 260 nm with a heating rate of 1.0 °C/min on a spectrophotometer (DU-640; Beckman, USA) equipped with a temperature regulator and a six-cell holder. Data were collected from 25 °C to 100 °C at 1 °C intervals. Samples were adjusted to an approximate absorbance of 0.5 at 260 nm in 10 mM sodium phosphate (pH 6.0) containing 50 mM NaCl. The solution was degassed under vacuum prior to collecting melting data.

Results and discussion

Imino proton resonances for each RNA sample were assigned based on the NOE connectivity (Fig. S1) and, as a result, their secondary structures were analyzed (Fig. S2). Mutation

of C8 to uridine (C8U) or adenosine (C8A) did not alter the structure of the U-U mismatch and the bulge. In contrast, substitution of C8 with guanosine (C8G) alters the structure of the U-U mismatch and/or single bulge to form the G-U mismatch and a U bulge. Mutant with deletion of C8 (C8del), insertion of another C in the bulge (C8CC) or formation of the U10-A28 base pair (U28A) formed the expected secondary structure.

The thermal stability of LINE36 and its mutants were analyzed by measuring the UV melting points (Table S1). The C8U or C8A mutation, which did not alter the secondary structure, showed only small change in the T_m value. On the other hand, C8del (deleting the bulge) or U28A (forming a U-A base pair instead of a U-U mismatch) significantly increased the T_m value. The C8G having the altered secondary structure showed 2.9 degree higher T_m value and the C8CC showed 3.5 degree lower T_m value. By comparing the T_m values with the retrotransposition activities, it seems that the appropriate thermal stability may be required for the efficient retrotransposition activity.

The effects of mutations on the retrotranspotition activities were discussed in the manuscript.

Figure legends

Fig. S1. 2D NOESY spectra of LINE36 (A) and its mutants C8U (B), C8A (C), C8G (D), C8del (E), C8CC (F) and U28A (G). The NOESY spectra (mixing time = 150 ms) were recorded at 4 °C, except for C8G and C8del at 10 °C.

Fig. S2. Secondary structures of the mutants were determined by NMR data. The mutated residues and deleted residue were indicated by open characters and open square, respectively. LINE36 (A), C8U (B), C8A (C), C8G (D), C8del (E), C8CC (F) and U28A (G) were shown.

Table S1. T_m values and retrotransposition frequency (RF) of LINE36 and its mutants.

	T_m (°C)	Δ T_m (°C)	RF (%)
LINE36	58.2	0.0	100
C8U	57.9	-0.3	~67
C8A	59.3	1.1	120
C8G	61.1	2.9	~4
C8del	63.8	5.6	~3
C8CC	54.3	-3.5	~15
U28A	67.7	9.5	~9

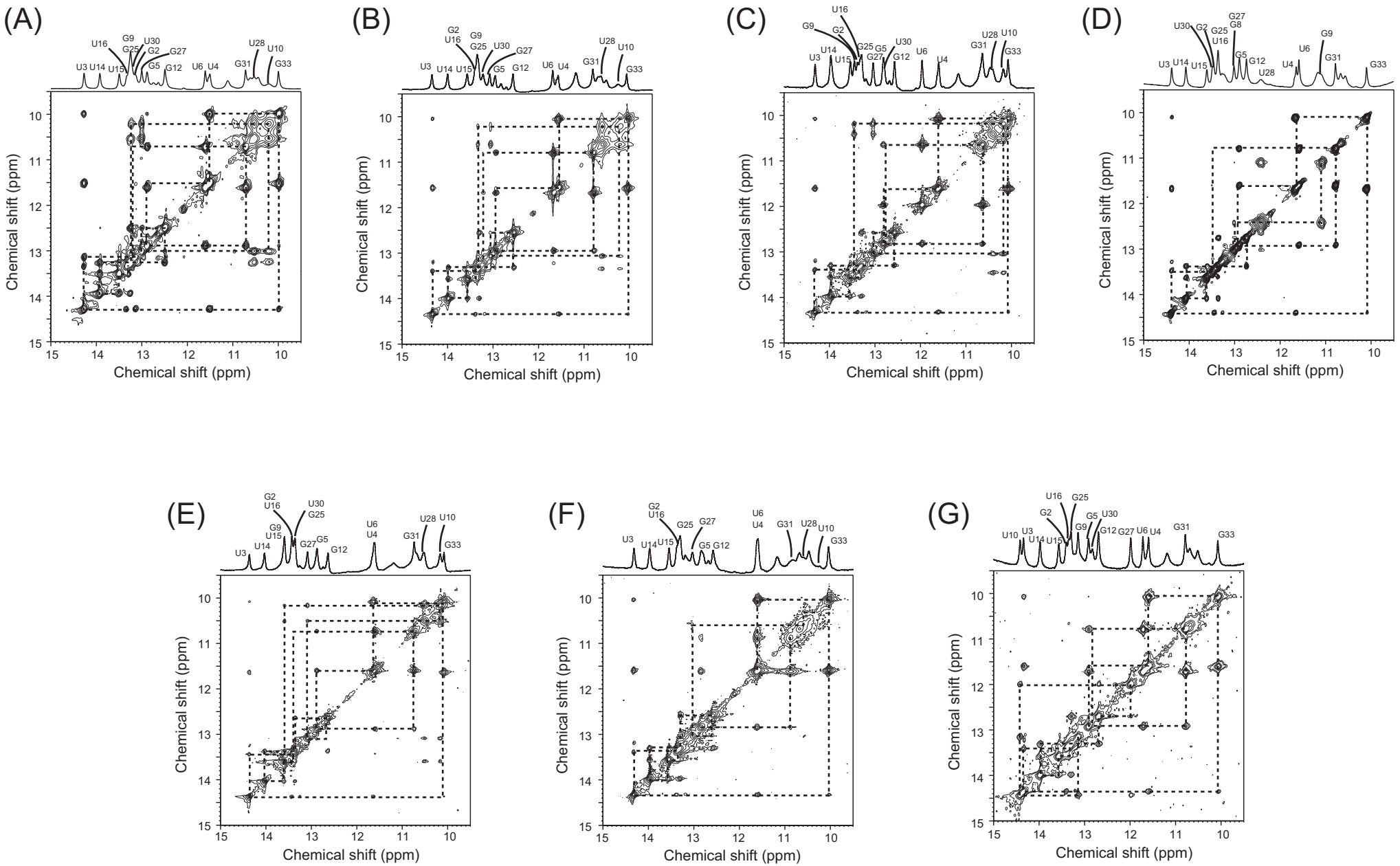

Figure. S1.

Nomura et al.

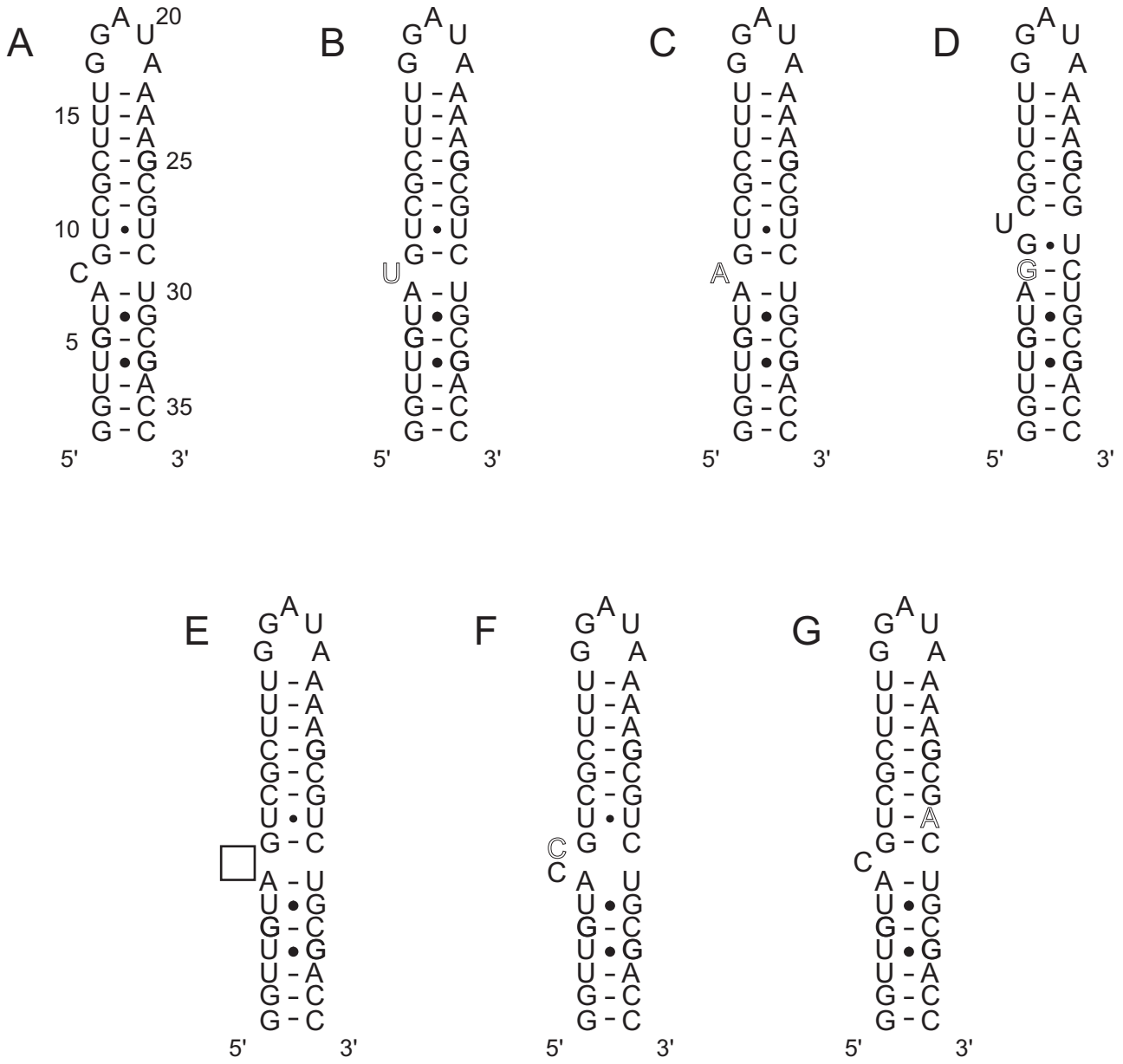

Figure. S2.

Nomura et al.

2. Supplemental figures and tables

Fig. S3. Sequential assignment of LINE36. The NOESY spectrum (mixing time = 400 ms) was recorded at 20 °C in D_2O, and cross peaks between aromatic H6 and H8 protons and ribose H1′ protons are shown. Sequential connectivities are indicated by lines, and intra-residue NOEs are labeled by residues.

Fig. S4. Graphs of energy during equilibration (a) and simulation (b) stage of the LINE36 molecular dynamics simulation. Equilibration was performed with 100 steps of minimization and 130 ps simulation. Temperature was warmed from 0 to 298 K over 20 ps with constant volume. Second phase, simulation was performed 20 ps with constant pressure and 0.2 ps pressure relaxation time. Third phase, simulation was performed 30 ps with constant pressure and 2.0 ps pressure relaxation time. These simulation was performed with 5.0 kcal/mol·Å RNA conformational constraint. Finally, simulation was performed 60 ps with reduced RNA conformational constraint from 1.0 to 0.1 kcal/mol·Å. Total energy for the whole system during equilibration stage is shown in Figure S4a, indicating that the simulation system was reached equilibrium state. The simulation was performed for 8 ns at constant volume and with periodic boundary conditions at 298 K. Total energy for the RNA molecule during molecular dynamics stage is shown in Figure S4b, indicating that the RNA molecule was reached equilibrium state. Thus, structural analyses of the trajectories from 3 ns to 8 ns were performed using the CARNAL module.

Table S2. Distance restraints based on the absence of NOE.

H2 (A19) – H1′ (A22)
H2 (A19) – H2 (A22)
H2 (A21) – H2 (A22)
H2 (A21) – H1′ (G17)
H8 (G17) – H2 (A22)
H1′ (G17) – H2′ (G18)
H1′ (A7) – H6 (C8)

Table S3. Effect of the database potential on the structural calculation.

database potential	without	with
RDC r.m.s.d.	1.60	1.72
r.m.s. deviations from experimental restraints		
Distance (Å)	0.0362 ± 0.0046	0.0387 ± 0.0013
Dihedral (°)	1.0778 ± 0.1120	0.2353 ± 0.1966
r.m.s. deviations from the idealized geometry		
Bonds (Å)	0.0061 ± 0.0002	0.0064 ± 0.0001
Angle (°)	2.4287 ± 0.0918	2.5077 ± 0.0115
Impropers (°)	1.8080 ± 0.1222	1.8760 ± 0.1089
Heavy-atoms r.m.s. deviation (Å)		
Upper stem	1.25	0.78
Lower stem	1.05	0.77

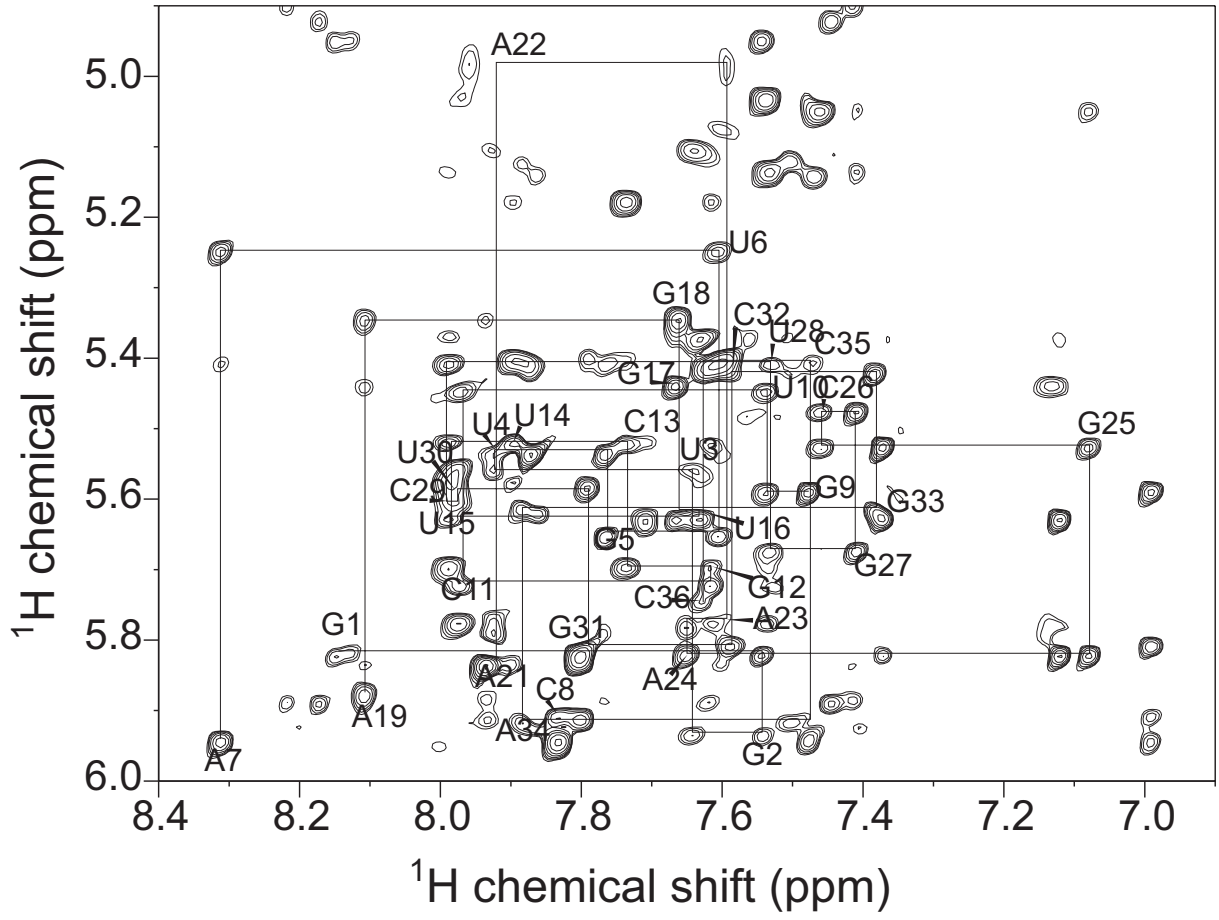

Figure. S3.

Nomura et al.

a)

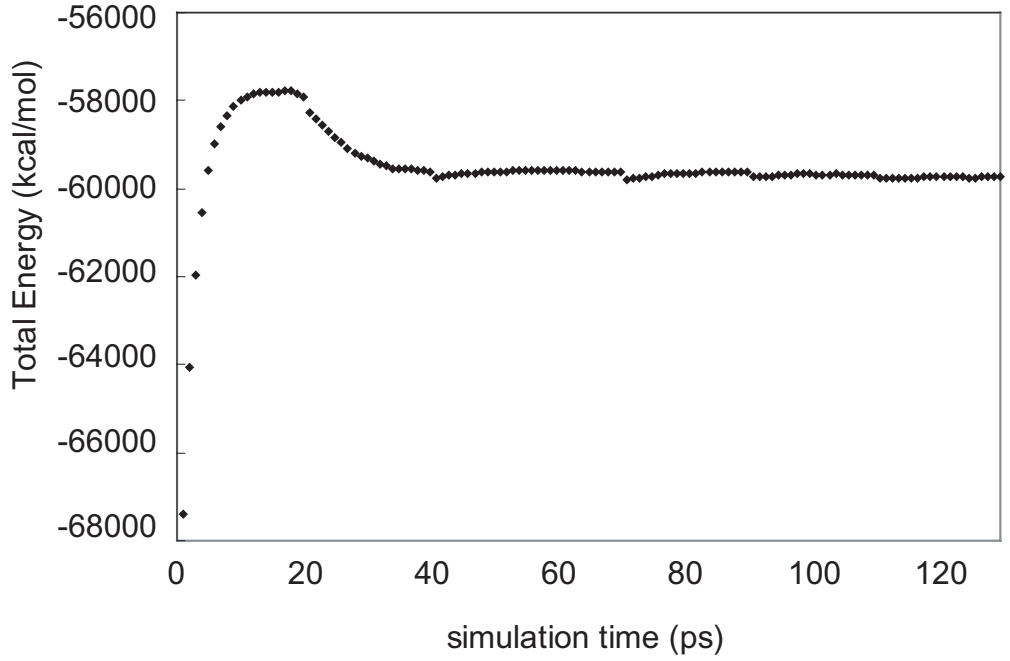

b)

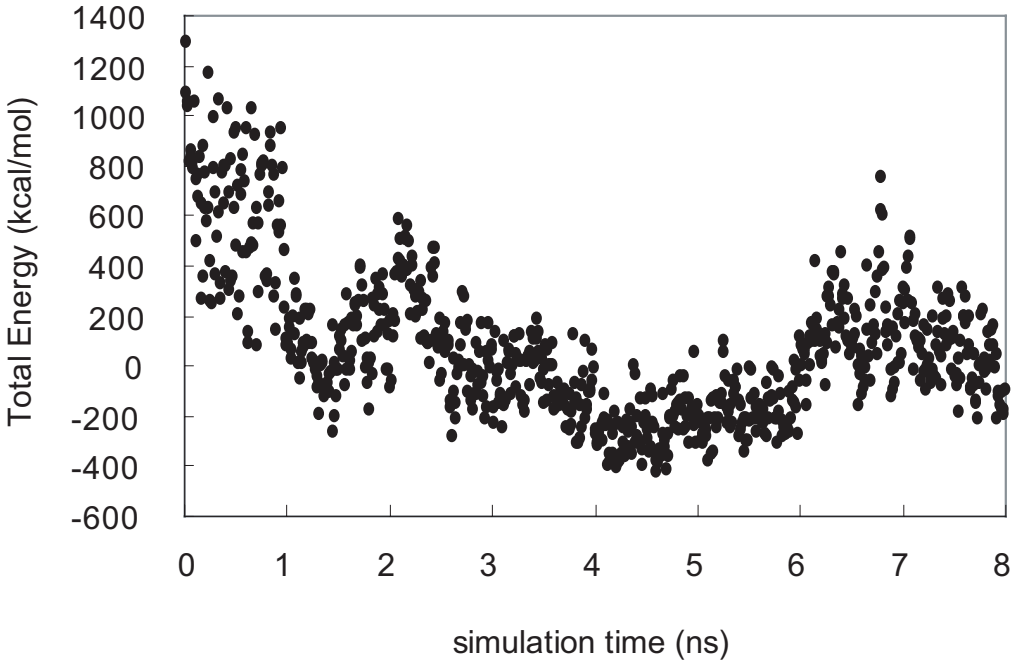

Figure. S4.

Nomura et al.